Research Article Vol. 24, No. 17 | 22 Aug 2016 | OPTICS EXPRESS 19558

Optics EXPRESS

Narrowband cw injection seeded high power femtosecond double-pass optical parametric generator at 43 MHz: Gain and noise dynamics

HEIKO LINNENBANK,* TOBIAS STEINLE, AND HARALD GIESSEN

4th Physics Institute and Research Center SCOPE, University of Stuttgart, 70550 Stuttgart, Germany
*h.linnenbank@pi4.uni-stuttgart.de

Abstract: We demonstrate narrowband cw injection seeding of a femtosecond double-pass optical parametric generator at 43 MHz repetition rate with a simple, low power external cavity diode laser. Up to 2.5 W of near-IR radiation (1.5 – 1.66 µm) as well as 800 mW of tunable mid-IR radiation (2.75 – 3.15 µm) with pulse durations below 300 fs are generated with a remarkable pulse-to-pulse and long term power stability. Compared to conventional, vacuum noise seeded optical parametric generators, the presented frequency conversion scheme does not only exhibit superior gain and noise dynamics, but also a high degree of flexibility upon control parameters such as pump power, seed power, or spectral position of the seed.

OCIS codes: (190.4360) Nonlinear optics, devices; (190.4975) Parametric processes; (190.4970) Parametric oscillators and amplifiers.

References and links

1. A. Schliesser, N. Picqué, and T. W. Hänsch, "Mid-infrared frequency combs," Nat. Photonics **6**(7), 440–449 (2012).
2. A. H. Zewail, Femtochemistry: *Ultrafast Dynamics of the Chemical Bond* (World Scientific, 1994).
3. J.-C. Diels and W. Rudolph, *Ultrashort Laser Pulse Phenomena,* 2nd ed. (Elsevier Inc., 2006).
4. D. Yelin and Y. Silberberg, "Laser scanning third-harmonic-generation microscopy in biology," Opt. Express **5**(8), 169–175 (1999).
5. C. H. Camp, Jr. and M. T. Cicerone, "Chemically sensitive bioimaging with coherent Raman scattering," Nat. Photonics **9**(5), 295–305 (2015).
6. S. V. Marchese, E. Innerhofer, R. Paschotta, S. Kurimura, K. Kitamura, G. Arisholm, and U. Keller, "Room temperature femtosecond optical parametric generation in MgO-doped stoichiometric $LiTaO_3$," J. Appl. Phys.-B **81**(8), 1049–1052 (2005).
7. T. W. Neely, T. A. Johnson, and S. A. Diddams, "High-power broadband laser source tunable from 3.0 µm to 4.4 µm based on a femtosecond Yb:fiber oscillator," Opt. Lett. **36**(20), 4020–4022 (2011).
8. K. C. Burr, C. L. Tang, M. A. Arbore, and M. M. Fejer, "High-repetition-rate femtosecond optical parametric oscillator based on periodically poled lithium niobate," Appl. Phys. Lett. **70**(25), 3341 (1997).
9. T. Steinle, A. Steinmann, R. Hegenbarth, and H. Giessen, "Watt-level optical parametric amplifier at 42 MHz tunable from 1.35 to 4.5 µm coherently seeded with solitons," Opt. Express **22**(8), 9567–9573 (2014).
10. F. Mörz, T. Steinle, A. Steinmann, and H. Giessen, "Multi-Watt femtosecond optical parametric master oscillator power amplifier at 43 MHz," Opt. Express **23**(18), 23960–23967 (2015).
11. C. Manzoni, G. Cirmi, D. Brida, S. de Silvestri, and G. Cerullo, "Optical-parametric-generation process driven by femtosecond pulses: Timing and carrier-envelope phase properties," Phys. Rev. A **79**(3), 033818 (2009).
12. H. Linnenbank and S. Linden, "High repetition rate femtosecond double pass optical parametric generator with more than 2 W tunable output in the NIR," Opt. Express **22**(15), 18072–18077 (2014).
13. M. Marangoni, R. Osellame, R. Ramponi, G. Cerullo, A. Steinmann, and U. Morgner, "Near-infrared optical parametric amplifier at 1 MHz directly pumped by a femtosecond oscillator," Opt. Lett. **32**(11), 1489–1491 (2007).
14. X. Xie, A. M. Schober, C. Langrock, R. V. Roussev, J. R. Kurz, and M. M. Fejer, "Picojoule threshold, picosecond optical parametric generation in reverse proton-exchanged lithium niobate waveguides," J. Opt. Soc. Am. B **21**(7), 1397–1402 (2004).
15. P. Zhao, B. Zhang, E. Li, R. Zhou, D. Xu, Y. Lu, T. Zhang, F. Ji, X. Zhu, P. Wang, and J. Yao, "Experimental study on a high conversion efficiency, low threshold, high-repetition-rate periodically poled lithium niobate optical parametric generator," Opt. Express **14**(16), 7224–7229 (2006).
16. M. Levenius, V. Pasiskevicius, F. Laurell, and K. Gallo, "Ultra-broadband optical parametric generation in periodically poled stoichiometric $LiTaO_{3,}$" Opt. Express **19**(5), 4121–4128 (2011).
17. J. E. Bjorkholm and H. G. Danielmeyer, "Frequency control of a pulsed optical parametric oscillator by radiation injection," Appl. Phys. Lett. **15**(6), 171 (1969).

#266737 http://dx.doi.org/10.1364/OE.24.019558
Journal © 2016 Received 30 May 2016; revised 4 Aug 2016; accepted 5 Aug 2016; published 15 Aug 2016

18. B. Köhler, U. Bäder, A. Nebel, J.-P. Meyn, and R. Wallenstein, “A 9.5-W 82-MHz-repetition-rate picoseconds optical parametric generator with cw diode laser injection seeding,” Appl. Phys. B **75**(1), 31–34 (2002).
19. L. Xu, H.-Y. Chan, S.-U. Alam, D. J. Richardson, and D. P. Shepherd, “High-energy, near- and mid-IR picosecond pulses generated by a fiber-MOPA-pumped optical parametric generator and amplifier,” Opt. Express **23**(10), 12613–12618 (2015).
20. T. Südmeyer, J. A. Au, R. Paschotta, U. Keller, P. G. R. Smith, G. W. Ross, and D. C. Hanna, “Novel ultrafast parametric systems: high repetition rate single-pass OPG and fibre-feedback OPO,” J. Phys. D Appl. Phys. **34**(16), 2433–2439 (2001).
21. S. T. Yang and S. P. Velsko, “Frequency-agile kilohertz repetition-rate optical parametric oscillator based on periodically poled lithium niobate,” Opt. Lett. **24**(3), 133–135 (1999).
22. C. W. Hsu and C. C. Yang, “Broadband infrared generation with noncollinear optical parametric processes on periodically poled $LiNbO_3$,” Opt. Lett. **26**(18), 1412–1414 (2001).
23. G. Arisholm, “General analysis of group velocity effects in collinear optical parametric amplifiers and generators,” Opt. Express **15**(10), 6513–6527 (2007).
24. R. W. Boyd, *Nonlinear Optics* (Third Edition) (Elsevier Inc., 2008).

1. Introduction

Both the mid-infrared as well as the near-infrared spectral region are highly interesting for spectroscopic applications. While the mid-infrared offers the opportunity to study vibrations of molecules and solids [1], near-infrared excitation provides the basis of time-resolved spectroscopy [2], multi-photon fluorescence [3], harmonic generation [4], and coherent Raman scattering microscopy [5] in biomedical investigations. For these applications, stable, coherent, high repetition rate femtosecond light sources with high peak intensities along with a broadband tunability are required. Femtosecond pulse lasers with several tens of Megahertz repetition rates would be an ideal choice, despite their limited tuning range and available center wavelengths. The recent development of high average power passively mode-locked solid state and fiber lasers allow direct pumping of optical parametric frequency down-conversion schemes, i.e., optical parametric oscillators (OPOs), optical parametric amplifiers (OPAs), and optical parametric generators (OPGs), which do not only generate a broadly tunable, but also intrinsically synchronized outputs in the desired spectral regions [6–8].

While femtosecond OPOs need rather complex cavities, which have to be synchronized to the pump laser and stabilized, OPAs demand for a seed source, which covers the desired spectral range, possess a high stability and also require to be synchronized to the pump laser [7,9,10]. OPGs, the simplest realization of optical parametric down conversion, do not have these disadvantages, but as OPGs are essentially equivalent to OPAs seeded by vacuum fluctuations, a high gain is necessary to generate a signal and the signal will be strongly fluctuating. However, it was shown that the fluctuation can be suppressed by driving the parametric process close to or into saturation [11–13]. For the parametric gain, two limiting factors can be perceived, namely the interaction length in the nonlinear crystal, constituted by the group velocity mismatch (GVM) of the signal and the idler pulses with respect to the pump pulse, that leads to a temporal walk off, as well as the damage threshold of the nonlinear crystal. The temporal walk off can be reduced by operating in a spectral range where the GVMs are nearly equal but antiparallel [11] or by using of a double-pass configuration where the temporal walk off is compensated between two passes through the crystal. As thermal loading is believed to be the main damage mechanism at high repetition rates, the damage threshold can be increased by a reduction of the repetition rate [14–16]. However, for various applications a high repetition rate is highly desirable.

To overcome these issues and to further suppress the output fluctuations as well as to lower the threshold of the previous high power double-pass OPG design [12], in this paper we combine the simple and reliable setup with a low power narrowband cw external cavity diode laser, which is tunable in the signal range of the OPG. The idea behind this so-called injection seeding is [17,18] as follows: Even if the power per pump pulse injected into the system by the cw diode laser was only on the order of the vacuum noise, which is not the case, it will still stabilize the output power of the system. However, the injected radiation is not just amplified by the OPG, which would strongly limit its spectral bandwidth [18,19], but only acts as starting mechanism for the parametric generation. Thus the spectral and temporal dynamics are dominated rather by the OPG process.

Optics EXPRESS

2. Experimental setup

The scheme of the narrowband cw injection seeded OPG, consisting of a double-pass OPG and the seeding unit, is shown in Fig. 1. An 8 W Yb:KGW oscillator [NT&C Yb:KGW 1040-8] delivering 400 fs pulses with 43 MHz repetition rate and a central wavelength of 1030 nm is used as pump source A half-wave plate and a Faraday isolator are used in combination as variable attenuator. The pump beam is focused to a diameter of 280 µm inside a periodically poled 10 mm long, 0.5 mm thick 5% MgO doped $LiNbO_3$ crystal (Covesion Ltd.). Such weak focusing was chosen to make use of the largest possible average pump power, whereas even weaker focusing would lead to diffraction at the crystals surfaces. The pump beam is reflected into the crystal by a long pass filter (LPF_1) at 1.2 µm wavelength with high suppression ratio. After passing the crystal, the beam is separated from the generated signal beam by an identical filter. For the second pass, the pump and the signal beams are retroreflected and focused into the crystal by broadband dielectric concave mirrors (DCM_1: reflection band 750-1100 nm; DCM_2: reflection band 1.28-1.9 µm), whereas DCM_2 can be precisely translated to ensure the temporal overlap in the second pass. Both dielectric concave mirrors are transparent for the idler radiation, therefore the idler light generated in the first pass will be lost. After the second pass, the amplified signal and the generated idler beam pass the long pass filter LPF_1, and they are collimated by a CaF_2 lens and separated by a dielectric 2.4 µm long pass filter (LPF_2) with large suppression ratio. The use of long pass filters with high optical density instead of dichroic mirrors suppresses all parasitic generated visible and residual pump light and thus avoids the need of subsequent filtering, particularly when compared with our previous setup [12]. Due to the use of an uncoated CaF_2 lens and long pass filters (LPF_1) employing UV grade fused silica as substrate, both the signal and the idler radiation will experience avoidable losses, which are not taken into account.

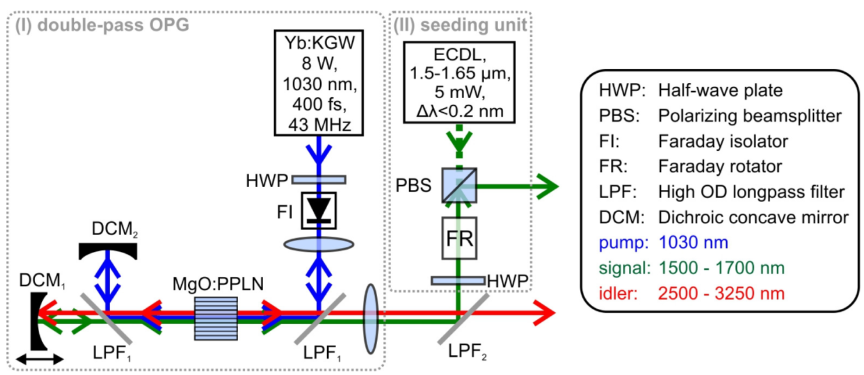

Fig. 1. Experimental setup consisting of (I) a double-pass OPG pumped by an Yb:KGW high power oscillator and (II) the seeding unit with of a narrowband, low power cw external cavity diode laser (ECDL) and a Faraday rotator combined with a polarizing beamsplitter to separate the seed from the signal output.

As narrowband cw seed source we utilize a fiber coupled external cavity diode laser (ECDL) in Littrow configuration, tunable between 1.5 µm and 1.65 µm and with up to 5 mW power at the fiber output in the gain maximum. The seed injection is accomplished by Faraday rotation. Here, the p-polarized seed passes the polarizing beam splitter and experiences a polarization rotation by 45° through the Faraday rotator, which is afterwards compensated by a half-wave plate. In contrast, for the signal radiation of the OPG the Faraday rotator acts in the same direction as the half wave plate, thus, by passing both, it is converted to s-polarized light and reflected by the polarizing beam splitter. The seeding unit introduces losses of 13% for the generated signal, which are not taken into account, although they are avoidable for an OPG without seeding unit.

3. Experimental results

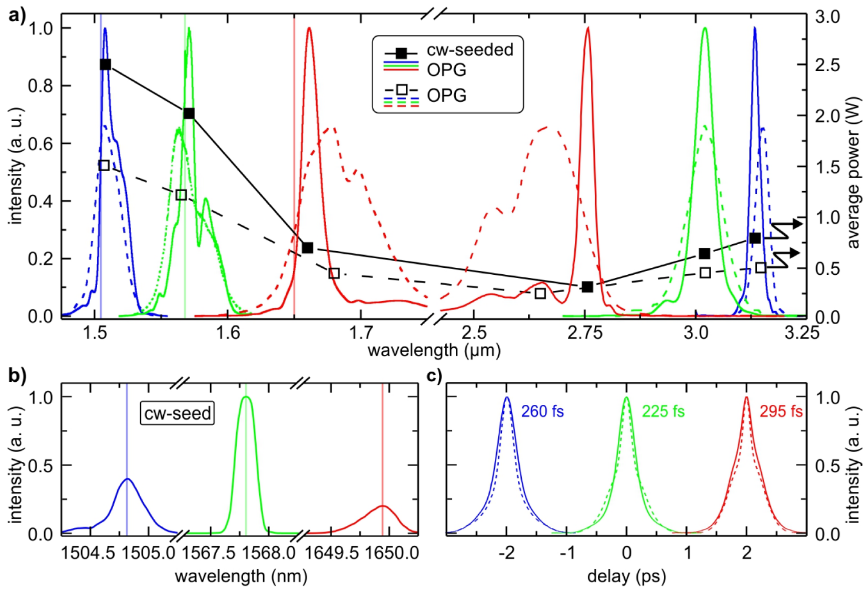

Fig. 2. (a) Tuning range (left axis) and average output power (right axis) of both the double-pass OPG without seed (dashed lines and open squares) and with narrowband cw injection seeding (continuous lines and filled squares) for different poling periods of 30 µm (blue), 30.5 µm (green), and 31 µm (red). (b) Spectra of the ECDL used as seed for the measurements depicted in (a). The peak level indicates the utilized seed power as 2 mW (blue), 5 mW (green), and 1 mW (red). The dim lines indicate the corresponding spectral positions of subfigures (a) and (b). (c) Intensity autocorrelation traces of the signal spectra depicted in (a), plotted in the same way. The FWHM pulse durations are given for the longer pulses, i.e., those generated with the cw injection seeded OPG, assuming sech2-pulse shapes. All measurements were taken at a constant pump power of 6.2 W.

The resulting spectra as well as the average output power of the OPG with cw injection seeding (continuous lines and filled squares) and without seeding (dashed lines and open squares) are shown in Fig. 2(a). Here, a constant pump power of 6.2 W and fixed poling periods of 30 µm (blue curves), 30.5 µm (green curves), and 31 µm (red curves) at room temperature have been used. Here, and in the following, the pump power is measured between the Faraday isolator and the pump focusing lens. The idler power is measured after the 2.4 µm long pass filter (LPF_2) and the signal power is measured after reflection by the polarizing beam splitter in the seeding unit. All values are quoted as measured, without taking into account the losses of the various optics. The double-pass OPG itself shows a remarkable performance, generating up to 1.2 W of average power in the signal and up to 500 mW in the idler spectral range. The investigated spectral range, namely 1.5 µm to 1.7 µm and 2.5 µm to 3.15 µm is limited by the tuning range of our current narrowband cw ECDL and is somewhat inconvenient, as the GVM of the signal and the idler pulses with respect to the pump pulse are both nonzero and parallel [11,14]. Even higher signal output powers up to 2.5 W and up to 800 mW in the idler range can be generated *with the cw injection seeded* double-pass OPG. Quite similar enhancement factors of 1.66 for the 30 µm and 30.5 µm and 1.56 for the 31 µm poling period for the signal generation and 1.6, 1.41, and 1.26, respectively, for the idler generation are achieved, despite the non-uniform utilized seed powers of 2 mW, 5 mW, and 1 mW for the 30 µm, 30.5 µm, and 31 µm poling periods, respectively, indicated by the different peak level of the cw seed spectra in Fig. 2(b). From the resolution limited shape of the cw seed spectra one can also perceive that at 1567.8 nm single-mode operation is achieved for the ECDL, while the bandwidth remains below 0.2 nm at the edges of the tuning range. Its center wavelengths is only in coincidence with the OPG (corresponding spectral positions of Fig. 2(a) and 2(b) are marked by dim lines) for the 30 µm and 30.5 µm poling period.

A slight narrowing by a factor of 1.3 due to cw seeding can be observed for the spectra of 30 µm and 30.5 µm poling periods, whereas a factor of 4 is measured for 31 µm poling period together with a spectral shift towards the center wavelength of the seed. Still the width of the spectrum displays the same order of magnitude as in the unseeded case and is thus more than 100 times broader than the seed spectrum. By this it becomes evident that the cw seed acts indeed only as injection source to initiate the OPG process.

In Fig. 2(c) the resulting signal intensity autocorrelation traces are depicted, exhibiting FWHM values below 300 fs when assuming sech^2 pulse shapes. In agreement with the spectral narrowing, the pulse durations of the unseeded OPG are slightly shorter than in the seeded case, but the relative difference of the pulse durations is less than that of the spectra, thus the time bandwidth (TBWP) product is enhanced. However, the autocorrelation traces as well as the signal spectra do not show clean Gaussian or sech^2 shapes as is known from strongly pumped OPGs [6,20].

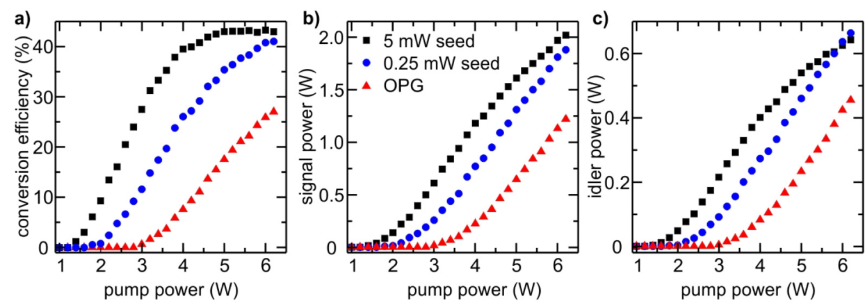

Fig. 3. (a) Total conversion efficiency, i.e., the ratio of the sum of signal and idler power and the average incident pump power versus the average incident pump power of the OPG without seeding (red triangles), with 5 mW (black squares), and 0.25 mW (blue circles) cw injection seeding at a wavelength of approximately 1570 nm (green spectra in Fig. 2(a)). (b) and (c) depict average output powers of the generated signal and idler radiation, respectively.

In the following a more detailed analysis of the performance and dynamics is performed for a cw seed wavelength of 1567.8 nm using the 30.5 µm period, i.e., the green curves in Fig. 2, for the case of 5 mW cw seed (black), 0.25 mW seed (blue), and for the unseeded OPG operation (red). Figure 3(a) shows the total conversion efficiency, which we define as the sum of the measured average signal and idler power, divided by the average incident pump power, as function of the average incident pump power. More than 40% conversion efficiency are achieved for both seed powers, whereas in the unseeded case only 28% efficiency are achieved. The conversion efficiency is linearly increasing with the pump power for 1.6 W - 4 W, 2.2 W - 4.8 W and 3.4 W - 6.2 W for 5 mW cw seed, 0.25 mW cw seed and the unseeded OPG, respectively. Thus, the operation threshold is strongly lowered by cw injection seeding. Saturation of the conversion efficiency is achieved, even in this somewhat unfavorable spectral region. However, a change of the seed power by a factor of 20 only leads to a moderate change in the average signal and idler output power (depicted in Fig. 3(b) and 3(c)), compared to the unseeded case, thus the employed seed power is a rather uncritical setting parameter for the presented system. This is due to the fact that for higher seed powers the conversion is just driven further into saturation. Hereby, an increasing part of the conversion is taking part in the first pass, which can be clearly seen in the case of the idler. At high pump powers even more idler power is generated with less seed, which is due to the fact that the idler radiation generated in the first pass is lost in our OPG scheme. The utilized seed powers relate to an effective seed per pump pulse of 80 fW and 4 fW, thus the double-pass OPG exhibits a gain of 104 dB and 107 dB, respectively.

The evolution of the generated signal autocorrelation traces and spectra are compared in Fig. 4(a)-4(e) and 4(f)-4(j), for approximately the same signal output power. Here, the autocorrelation traces for the case of cw seeding are nearly indistinguishable, especially at low output powers. Therefore, the FWHM pulse widths assuming $sech^2$ pulse shapes are only given for 5 mW seed and for the unseeded OPG. The unseeded OPG always exhibits somewhat smaller FWHM values, yet a deformation of the pulse shape occurs already at 450 mW signal power, manifested by a broadening of the side wings. Such a broadening becomes also visible in the seeded case but is by far weaker, despite for 1500 mW signal power, which however cannot be generated with the unseeded OPG. This pulse distortion seems to be also weaker for a stronger cw seed. While the pulse widths are monotonously decreasing up to 1200 mW signal power, an increase can be recognized at 1500 mW, followed again by a decrease for 2000 mW (see Fig. 2(c)).

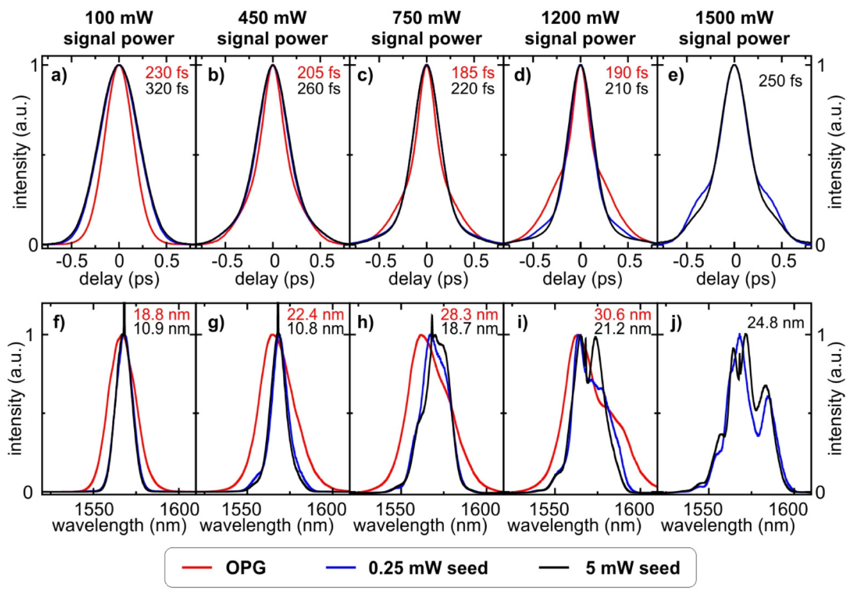

Fig. 4. (a-e) Intensity autocorrelation traces and (f-j) corresponding spectra of the signal radiation of the OPG without seeding (red), with 5 mW (black), and 0.25 mW (blue) cw injection seeding for signal powers of approximately 100 mW (a and f), 450 mW (b and g), 750 mW (c and h), 1200 mW (d and i), and 1500 mW (e and j). The FWHM values of the spectra are given for the OPG without seeding (red values) and with 5 mW cw injection seeding (black values), as well as the corresponding pulse durations assuming $sech^2$-pulse shapes.

Unlike the autocorrelation traces, the FWHM values of the signal spectra of the unseeded OPG are significantly higher than in the seeded case. Only slight differences occur for different cw seed powers, resulting in a strong reduction of the TBWP, being as low as 0.33 at 450 mW signal power for the seeded and as low as 0.51 at 100 mW for the unseeded OPG. As the spectra and autocorrelation traces for the cw seeded OPG are rather weakly distorted up to 1200 mW signal power, a description by $sech^2$ shapes is reasonable which imply nearly Fourier limited pulses. In the unseeded case, the evolution of the spectra starts with a symmetric spectrum, which is broadened with increasing signal power, evolving into an asymmetric shape, consisting of the original peak and a second one at longer wavelengths. Both the broadening and the occurrence of a second peak are less pronounced for the cw seeded OPG, however a dip in spectrum close to the seed wavelength occurs at 1200 mW signal power. The longer wavelength peak can be explained by parasitic noncollinear phase matching [21,22], which is thus at least partly suppressed by injection seeding. To the contrary, the dip in spectrum of the seeded OPG could result from backconversion [23]. This is in agreement with the measurements presented in Fig. 3, as for both cw seed powers 1200 mW signal power correlates to the onset of saturation of the conversion efficiency, which is hence caused by backconversion. Recapitulating Fig. 3 and Fig. 4 we can conclude that through the injection of a few milliwatts and less of cw seed into the double-pass OPG at the same signal powers a much cleaner signal with respect to the temporal and spectral dynamics can be generated with a lower pump power consumption, while even higher signal powers can also be generated at the expense of signal quality due to backconversion.

An investigation into the noise dynamics of the signal output for both cases on different time scales is presented in Fig. 5. We restrict ourselves for the sake of clarity to 5 mW cw seeding and the unseeded OPG, for selected pump power levels. Figures 5(a) and 5(b) display the long term stability, measured with a thermal power meter over one hour, as well as typical pulse trains over one microsecond when our system is operated close to the operation threshold (left column), i.e., 100 mW of signal power (2 W and 3.4 W pump power respectively), and for the maximum pump power of 6.2 W (right column). Both, the long term and the pulse-to-pulse stability are significantly enhanced by injection of a few milliwatts cw seed. As the unseeded OPG already exhibits reasonable long term stability at the operation threshold and upon strong pumping, the stabilizing influence is more dramatic for the pulse-to-pulse fluctuation. Here, the OPG is highly unstable at the operation threshold and is at least somehow stabilized at strong pumping, whereas the cw seeded OPG shows a remarkable high pulse-to-pulse stability already at the operation threshold which seems to decrease marginally for high pump powers.

A more detailed investigation is performed by analyzing the noise power spectral density of the signal with a lock-in amplifier (Zurich-Instruments UHFLI), measured with a biased photo diode (G12182-010, Hamamatsu) leveled to a photocurrent of 1.3 mA and low-pass filtered at 20 MHz. The results are depicted in Fig. 5(c), wherein the increasing pump power levels are displayed by a transition from dotted to continuous lines. The unseeded OPG shows a rather frequency independent noise spectrum, which decreases from the operation threshold to 6.2 W pump power by 7 dB and preserves the same form. However, injection of the cw seed does not only dramatically enhance the stability by 20 dB and more at all frequencies and pump powers, but also leads to a different behavior in general. A monotonous decrease with increasing pump power can be seen for the low frequencies, but at high frequencies a strong decrease followed again by an increase becomes visible. We also performed additional measurements for case of 0.25 mW cw seed resulting in qualitatively the same curves, but shifted upwards by approximately 7 dB (not shown). The reasons for this effect are the different origins of the fluctuation. While the low frequency fluctuations are mainly caused by mechanical and thermal instabilities, as well as low frequency fluctuations of the pump and seed, we account the high frequency fluctuations to quantum-noise induced statistic fluctuations of pulse parameters, such as spectral and temporal shape of both signal and idler during the conversion process, impacting on the measured pulse energies. In the case of the unseeded OPG both seeds are low amplitude random noise, which is depleted by an increase of the pump power and thereby driving the gain closer to saturation. For the cw seeded OPG we can assume the signal seed to be constant and the idler seed to be strongly fluctuating on a short time scale but with a small amplitude. By solving now the coupled amplitude equations of optical parametric amplification [24], for the case of no idler amplitude and a small idler amplitude, one can anticipate an increase in the relative difference of the resulting signal amplitudes with increasing pump amplitude and decreasing signal seed. This description corresponds well to findings, if we account the results at 2 W pump power to general instabilities at the operation threshold.

Optics EXPRESS

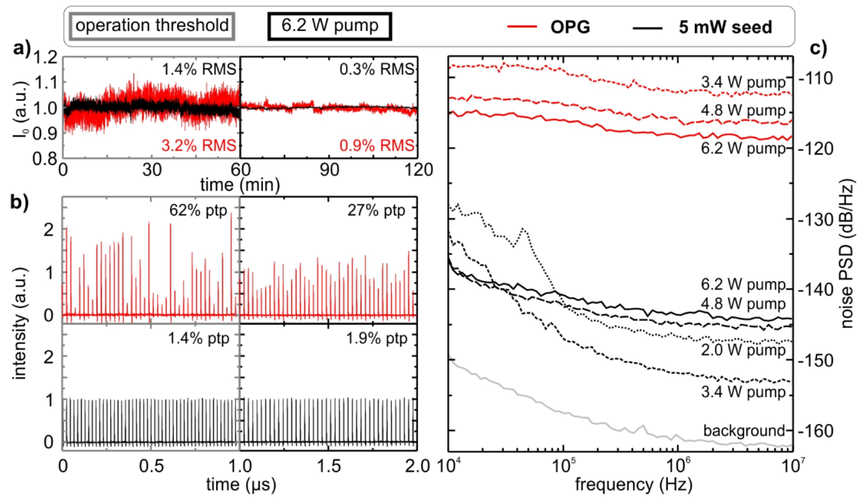

Fig. 5. (a) Long term average power stability recorded over one hour of the OPG without seeding (red traces) and with 5 mW cw injection seeding (black traces) slightly above the operation threshold (grey axes), i.e., at 3.4 W pump power and 2.0 W pump power, respectively, and at 6.2 W pump power (black axes). (b) Pulse-to-pulse stability over 1 µs for the same conditions as in subfigure (a). (c) Intensity noise spectrum of the OPG without seeding (red traces) and with 5 mW cw injection seeding (black traces) for pump powers increasing from 2 W to 6.2 W (dotted to solid lines), measured at 1.3 mA photocurrent. The detection electronic background is displayed in grey.

At first glance, the rise of the high frequency noise with increasing pump power in the case of the cw seeded OPG seems to be a drawback of by injection seeding, however, compared to the unseeded OPG [11,12] and also to conventional white light seeded OPAs [7,9], a quite high degree of stability is reached. We actually showed in the discussion of the spectral and temporal dynamics that a too high gain, achieved by strong pumping, is rather unfavorable due to distorting back conversion effects. Thus the injection of a weak cw seed leads, for comparable resulting signal powers where also temporal and spectral smooth, nearly Fourier limited pulses are generated, to a decrease of the high frequency noise by 35 dB. Moreover, stable operation is achieved even close to the operation threshold, where a pure OPG is nearly unusable.

4. Conclusion

We demonstrated experimentally that by injecting a few milliwatts of narrowband cw radiation from a tunable external cavity diode laser via Faraday rotation into a high power femtosecond double-pass OPG, operating at 43 MHz repetition rate, a dramatic enhancement of the overall system performance can be achieved. An enhancement of the average output power between 30% and 66% is achieved, both for signal and the idler spectral range, i.e., 1.5 µm to 1.65 µm and 2.5 µm to 3.15 µm, respectively, corresponding to average output powers of up to 2.5 W and 800 mW, respectively. As the cw seed only acts as starting mechanism for the parametric conversion, the generated output, i.e., the spectral bandwidth and pulse width, is still mainly constituted by the process of optical parametric generation and thus rather weakly affected by the setting parameters of cw seed laser, such as average power, spectral bandwidth, or exact center wavelength. The major advantage of cw seeding compared to the unseeded OPG is the dramatic suppression of both the long term and pulse-to-pulse fluctuations to below 2% in the entire operation regime and hence also at the operation threshold, where OPGs are usually unusable due to their strongly fluctuating output. This is especially of interest as the threshold is strongly lowered by cw injection seeding. Additionally, backconversion and parasitic noncollinear phase matching effects resulting from strong pumping which is used to suppress the intrinsic fluctuations can be circumvented.

Optics EXPRESS

Therefore a much cleaner signal with respect to the temporal and spectral dynamics can be generated with lower pump power consumption. As a low power tunable external cavity diode laser is employed as seed, we could still achieve nearly half the tuning range of unseeded OPGs pumped at one micrometer wavelength [12,20], while keeping the system rather simple compared to OPAs employing soliton/white-light sources, or even OPOs as seed [7,9,10].

Funding

ERC Advanced Grant (COMPLEXPLAS), DFG (SPP1391, FOR730 and GI 269/11-1), Bundesministerium für Bildung und Forschung (13N9048, 13N10146 and PRINTOPTICS), Carl Zeiss foundation, and Baden-Württemberg Stiftung (Spitzenforschung II), University of Stuttgart (open access fund).